Investigation of the causes of limit cycle saturation using a G–Equation model in the case of a laminar anchored flame in a simple combustor

Charles M. Luzzato, Aimee S. Morgans
Department of Aeronautics, Imperial College London, UK, Email: charles.luzzato@luzzato.com

Introduction

Combustion instabilities are caused by the interaction of acoustics and unsteady heat release. They lead to an increase in noise and structural loading, and are especially common in the lean–premixed fuel systems designed to reduce NO_x emissions. Understanding, preventing and suppressing these instabilities [1] is therefore a research priority.

Due to the complexity of real combustors, simple models of combustors containing an 'anchored ducted–flame' are commonly used in the first instance. These combine (i) a simple model of the acoustic wave behaviour with (ii) a flame model which captures how the flame responds to, and generates, acoustic waves. One of the most widely used flame models is the G–Equation model [2]. It models the kinematics of the flame non-linearly, capturing effects such as saturation into limit cycle, and showing reasonable agreement with experimental results [4, 6]. When implementing the G–Equation in anchored ducted-flame models, it has always previously been assumed that the discontinuity or "jump" in the acoustic wave strengths due the flame remains *immobile and at the flame anchor position*. This is despite the fact that the time-space average position of the flame is generally located a distance downstream of the anchor, and that furthermore the spatial-mean position of the flame oscillates in time.

The first improvement to the standard anchored ducted–flame model considered in this paper is to investigate the effect of using an acoustic wave strength discontinuity located at the time-space average position of the flame, rather than at the flame anchor. A further improvement is to allow the position of the acoustic waves strength discontinuity to vary in time, tracking the location of the spatial-mean position of the flame. This allows us to account for the direct effects of the flame movement on the acoustic source location. The discontinuity location alters the phase relationship between the acoustic pressure and unsteady heat release rate [9, 8], and so the effect of this change on combustor stability and, in cases of instability, limit cycle amplitude, is considered.

Review of the anchored ducted–flame model

We first review the anchored ducted–flame model in the form in which it has previously been used, before describing our improvements.

The model considers (i) the acoustic waves and (ii) the flame motion, coupling these via equations for the "jumps" or discontinuities in acoustic variables across the flame anchor position.

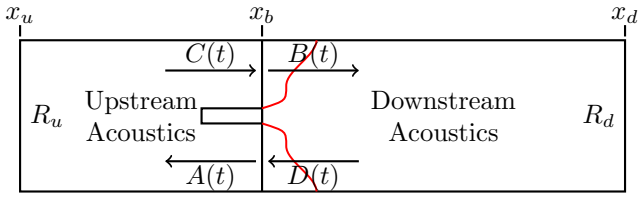

Figure 1: Schematic of the combustor duct, showing the incoming and outgoing pressure waves and the pressure reflection coefficients at the boundary. The discontinuity in acoustic wave strengths is positioned at the point where the flame is anchored to the flame holder: $x_b = 0\,\text{m}$.

Considering first the acoustic waves, the mean flow is considered uniform upstream and downstream of the flame, and the presence of vorticity or entropy waves neglected. The flow variables can be decomposed into a steady mean, and a small acoustic fluctuation: $(p(t,x), u(t,x), \rho(t,x)) = (\overline{P}, \overline{U}, \overline{\rho}) + (p_a(t,x), u_a(t,x), \rho_a(t,x))$, such that only linear fluctuations need be retained. Frequencies are assumed sufficiently low for only plane acoustic waves to exist - these can then be expressed using the method of characteristics [6], as shown in Figure 1.

Upstream of the flame–induced discontinuity ($_u$) the acoustic variables are [3]:

$$p_a(x,t) = C(t - \tau_{u_C}(x)) + A(t + \tau_{u_A}(x)) \quad \text{[Pa]} \quad (1)$$

$$u_a(x,t) = \frac{C(t - \tau_{u_C}(x)) - A(t + \tau_{u_A}(x))}{\overline{\rho}_u \overline{c}_u} \quad \text{[m/s]} \quad (2)$$

while downstream ($_d$):

$$p_a(x,t) = B(t - \tau_{d_B}(x)) + D(t + \tau_{d_D}(x)) \quad \text{[Pa]} \quad (3)$$

$$u_a(x,t) = \frac{B(t - \tau_{d_B}(x)) - D(t + \tau_{d_D}(x))}{\overline{\rho}_d \overline{c}_d} \quad \text{[m/s]} \quad (4)$$

where the density is $\rho_a(x,t) = \frac{p_a(x,t)}{\overline{c}^2}$ and $\overline{c}$ is the speed of sound. The time delays

$$\tau_{u_A}(x) = \frac{x - x_b}{\overline{c}_u - \overline{U}_u} \qquad \tau_{u_C}(x) = \frac{x - x_b}{\overline{c}_u + \overline{U}_u} \quad \text{[s]} \quad (5)$$

$$\tau_{d_B}(x) = \frac{x - x_b}{\overline{c}_d + \overline{U}_d} \qquad \tau_{d_D}(x) = \frac{x - x_b}{\overline{c}_d - \overline{U}_d} \quad \text{[s]} \quad (6)$$

represent:

- $\tau_{u_A}(x)$: the time taken for wave $A(t)$ to go from the discontinuity x_b to a point upstream x;

- $\tau_{u_C}(x)$: the time taken for wave $C(t)$ to go from a point upstream x to the discontinuity x_b;
- $\tau_{d_B}(x)$: the time taken for wave $B(t)$ to go from the discontinuity x_b to a point downstream x;
- $\tau_{d_D}(x)$: the time taken for wave $D(t)$ to go from a point downstream x to the discontinuity x_b.

Pressure reflection coefficients are used to impose physical behaviour at boundaries:

$$C\left(t-\tau_{u_C}\left(x_u\right)\right)=R_u A\left(t+\tau_{u_A}\left(x_u\right)\right) \quad \text{[Pa]} \quad (7)$$

$$D\left(t+\tau_{d_D}\left(x_d\right)\right)=R_d B\left(t+\tau_{d_B}\left(x_d\right)\right) \quad \text{[Pa]}. \quad (8)$$

The effects of the flame on the acoustics are imposed at the flame anchoring position. Wave strengths either side of the the anchor position are then related by imposing the flow conservation equations across the flame [7]. The conservation of energy means that the acoustics wave strengths are not constant across the flame, but rather experience a "jump" or discontinuity, which depends upon the total heat release rate, Q, of the flame [7].

A flame model is needed to capture the variation in $Q(t)$. The well-known G–Equation model assumes that the flame responds to the flow velocity directly upstream, its motion being governed by a non-linear partial differential equation: the G–Equation. This is derived by assuming that the flame initiation surface $\mathcal{G}$ is convected by its relative burning velocity $u_{\text{gutter}} - S_u \cdot \mathbf{n}$ ($\mathbf{n}$ being the unit normal to the flame), such that $\frac{D\mathcal{G}}{Dt} = 0$ [7]. The movement and shape of the flame are then tracked by considering $\mathcal{G} = x - \xi(t, r)$;

$$\frac{\partial \xi}{\partial t}=u_{\text{gutter}}-S_u\sqrt{1+\left(\frac{\partial \xi}{\partial r}\right)^2} \quad \text{[m/s]} \quad (9)$$

where u_{gutter} is the velocity just upstream of the discontinuity, r is the radial position in the duct, and S_u is the laminar burning velocity, usually chosen empirically. Anchoring of the flame is imposed through $\xi = 0$ at the anchor point (here $x = 0$). It is assumed that $Q(t) \propto \mathcal{A}(t-\tau_f)$, where τ_f is chosen empirically and the flame area $\mathcal{A}$ is given by:

$$\mathcal{A}(t)=\int_{r_a}^{r_b} 2\pi r\sqrt{1+\left(\frac{\partial \xi}{\partial r}\right)^2}\,dr \quad \left[\text{m}^2\right] \quad (10)$$

where r_a is the radius of the flame holder, and r_b is the radius of the duct. Thus at any point in time, the jump in the wave strengths either side of the flame depends on the flame area and hence the instantaneous flame shape.

Varying the discontinuity position

In the above, the position at which the flow conservation equations were applied and at which the acoustic waves experienced a discontinuity (x_b), was fixed in time at the flame anchoring position. For compact flames and small amplitude oscillations, this is usually a good approximation [3]. However, when the combustor is unstable, the amplitude of the flame motion can become large [5]. Then, even under the simplifying assumption that the heat release can be referred to as a single axial location (necessary when assuming plane acoustic waves), the flame–induced acoustic wave discontinuity should follow the spatial–mean flame position in time.

To account for the flame movement, the location of the acoustic wave discontinuity is now denoted $x_b(t)$, and the time delays (5) and (6) become:

$$\tau_{u_A}(x,t)=\frac{x-x_b(t)}{\overline{c}_u-\overline{U}_u} \quad \tau_{u_C}(x,t)=\frac{x-x_b(t)}{\overline{c}_u+\overline{U}_u} \quad \text{[s]} \quad (11)$$

$$\tau_{d_B}(x,t)=\frac{x-x_b(t)}{\overline{c}_d+\overline{U}_d} \quad \tau_{d_D}(x,t)=\frac{x-x_b(t)}{\overline{c}_d-\overline{U}_d} \quad \text{[s]} \quad (12)$$

$x_b(t)$ now tracks the average location of the heat release $x_f(t)$ in time, this being given by the area-weighted mean flame position (as $Q(t) \propto \mathcal{A}(t-\tau_f)$):

$$x_f(t)=\frac{\sum_{k=1}^{n}\mathcal{A}_k(t-\tau_f)\,\xi_k(t-\tau_f)}{\sum_{k=1}^{n}\mathcal{A}_k(t-\tau_f)} \quad \text{[m]}. \quad (13)$$

Here $\mathcal{A}_k$ is the incremental flame area at the discrete position ξ_k, computed in a similar fashion to (10) such that $\mathcal{A} = \sum_{k=1}^{n}\mathcal{A}_k$. Since $\mathcal{A}_k$ depends on the flame shape position ξ, it follows that $x_b(t+\tau_f)$ depends on the pressure waves $C(t)$ and $A(t)$ just ahead of the flame. That is, the acoustic wave strengths ahead of the flame depend on the flame position, but the flame position depends on these wave strengths. Thus the acoustic discontinuity location and flame are now coupled.

To overcome this problem, we know that waves $A(t)$ and $B(t)$, moving away from the discontinuity, are obtained directly from the jump equations, and are not part of the coupled problem (even if the location at which they are emitted is for now unknown). The strengths of waves C and D as they arrive at the discontinuity requires more work. From equation (7), it follows that $C(t)$ and $D(t)$ at $x_b(t)$ depend only on the outgoing wave strengths A and B at previous times $t-\tau_u$ and $t-\tau_d$, where

$$\tau_u=-\tau_{u_A}(x_u,t-\tau_u)-\tau_{u_C}(x_u,t) \quad \text{[s]} \quad (14)$$

$$\tau_d=\tau_{d_B}(x_d,t-\tau_d)+\tau_{d_D}(x_d,t) \quad \text{[s]}. \quad (15)$$

τ_u and τ_d represent the times taken for a wave to travel from the discontinuity to the boundary and back to the (changed position of the) discontinuity again. These two time delays depend on the values of x_b when A and B leave the discontinuity, $x_b(t-\tau_u)$ and $x_b(t-\tau_d)$, as well as $x_b(t)$ when C and D arrive back at the discontinuity.

Thus the waves $C(t)$ and $D(t)$, arriving at the discontinuity location $x_b(t)$, depend on x_b at three times: $x_b(t)$, $x_b(t-\tau_u)$ and $x_b(t-\tau_d)$. $x_b(t)$ depends, amongst other variables, on the upstream wave $C(t-\tau_f)$. As is common in moving acoustic source problems, such as those encountered in helicopter acoustics [10], the problem must be solved iteratively. This yields equations:

$$x_b(t)=f\left(u_{\text{gutter}}(t-\tau_f),\xi(t-\tau_f)\right) \quad \text{[m]} \quad (16)$$

$$\tau_{u_A}(x_u,t-\tau_u)=\frac{x_u-x_b(t-\tau_u)}{\overline{c}_u-\overline{U}_u} \quad \text{[s]} \quad (17)$$

$$\tau_{d_B}(x_d,t-\tau_d)=\frac{x_d-x_b(t-\tau_d)}{\overline{c}_d+\overline{U}_d} \quad \text{[s]} \quad (18)$$

Table 1: Combustor parameters for the test cases investigating combustor stability.

Case	x_u[m]	x_d[m]	x_{ref}[m]	R_u	R_d	M_u
1	-0.3	.841	0.33	-1	-1	0.08
2	-1.5	.6855	0.22	0.85	-.98	0.08

Table 2: Combustor dominant oscillation frequencies for the test cases investigating combustor stability.

	Frequencies [rad/s]		
Case	$x_b = 0$	$x_b = \overline{x}_f$	$x_b(t) = x_f(t)$
1	244	277	277
2	336	360	360

where $f(u_{\text{gutter}}, \xi)$ is a function including the area weighted mean (13) and the G–Equation (9).

Results

To investigate the effects of implementing the acoustic jump location more accurately, two sets of combustor test cases are considered. The first set is concerned with combustor stability, while the second set considers limit cycle amplitude. for both sets the upstream total temperature is $T_0 = 288\,\text{K}$, mean heat release rate is $\overline{Q} = 59\,\text{MJ m}^2/\text{s}$, downstream mean pressure is $\overline{P} = 1.013 \cdot 10^5$ Pa and duct dimensions are $r_a = 1.75\,\text{cm}$ and $r_b = 3.5\,\text{cm}$. We compare results for three discontinuity location implementations:

- the standard ducted–flame model with $x_b = 0$;
- the discontinuity position fixed at the space-time average flame position, $x_b = \overline{x}_f$;
- the discontinuity position moving in time to track the spatial-mean flame position, $x_b(t) = x_f(t)$.

Combustor stability

Two test cases are considered here, for which the combustor geometries, upstream Mach number and boundary reflection coefficients are shown in Table 1 (the normalised acoustic pressure, p_{ref}, at location x_{ref} is measured).

The resulting dominant oscillation frequencies are shown in Table 2. It is seen that accounting for the shift in the spatial-mean position of the flame gives rise to a frequency shift of up to 14%, due to the change in mode shape.

The envelopes of the corresponding pressure oscillations are shown in Figure 2. For both cases:

- $x_b = 0$ gives rise to an unstable system which quickly saturates into a limit cycle.
- $x_b = \overline{x}_f$ gives rise to an unstable system with a much lower oscillation amplitude (still slowly growing – true limit cycle saturation has not yet occurred)
- $x_b(t) = x_f(t)$ gives rise to a stable system whose oscillation amplitude is slowly decaying.

Thus accounting for the movement of the flame (by shifting the mean position at which the flame-induced discontinuity is assumed to occur) is seen to be important in accurately capturing the stability of the system in these test cases.

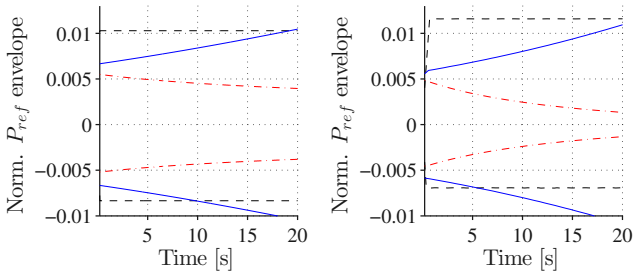

Figure 2: Envelope of the normalised pressure p_{ref}: - - - - - $x_b = 0$ (multiplied by a factor 1/6); ——$x_b = \overline{x}_f$; -·-·- $x_b(t) = x_f(t)$. Case 1 left, case 2 right.

Table 3: Combustor parameters for the test case investigating limit cycle amplitude.

x_u[m]	x_d[m]	x_{ref}[m]	R_u	R_d	M_u
-1.0	1.015	0.33	0.85	-.98	0.08

Limit cycle amplitude

For the test case chosen here, summarised by the parameters in Table 3, high amplitude limit cycle oscillations occur which give rise to large amplitude motion of the flame-induced discontinuity.

The dominant oscillation frequency is observed to be 320 rad/s using $x_b = 0$, 333 rad/s using $x_b = \overline{x}_f$ and 325 rad/s using $x_b(t) = x_f(t)$, again showing a significant shift depending on the location of the discontinuity. The envelopes of the corresponding pressure oscillations are shown in Figure 3. It can be observed that using $x_b(t) = x_f(t)$ leads to a substantial 47% decrease in negative peak amplitude when compared to the $x_b = \overline{x}_f$ case. This demonstrates that there are likely to be conditions under which accounting for flame movement, by changing the location of the acoustic discontinuity, is important in determining the limit cycle amplitude.

Discussion

To further understanding of why applying the acoustic jump location more accurately affects both stability and limit cycle amplitudes, the well-known Rayleigh source term, $p_a Q'$ (averaged over an oscillation cycle) is considered. It is well known from the Rayleigh criterion [9] that the larger this source term, the more likely it is to exceed loss terms and give rise to instability.

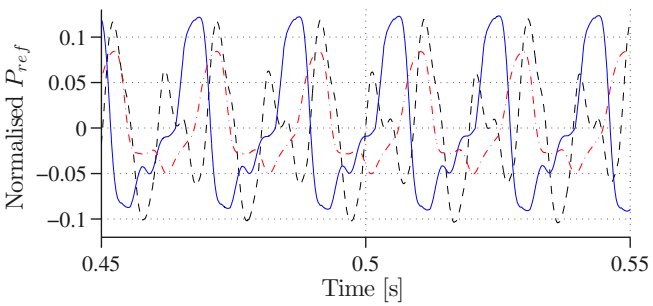

Figure 3: Normalised limit cycle pressure fluctuation, p_{ref}: - - - - - $x_b = 0$; ——$x_b = \overline{x}_f$; -·-·- $x_b(t) = x_f(t)$.

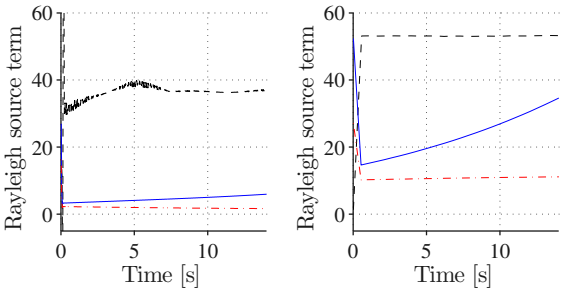

Figure 4: Normalised Rayleigh source term: ---- $x_b = 0$ (Cases 1 and 2 multiplied by factors 0.5 and 0.02 respectively); —— $x_b = \overline{x}_f$; -·-·- $x_b\,(t) = x_f\,(t)$. Case 1 left, case 2 right.

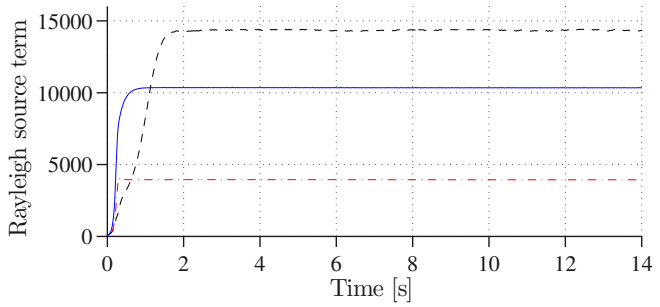

Figure 5: Normalised Rayleigh source term: ---- $x_b = 0$, —— $x_b = \overline{x}_f$ and -·-·- $x_b\,(t) = x_f\,(t)$ models.

For the combustor stability test cases (1 and 2), the time integrated source term product, $p_a Q'$, is shown in Figure 4. It can clearly be seen that changing the location of the flame-induced discontinuity alters this source term. In fact, it appears to be generally the case that accounting for flame movement about a given position, and therefore changing the position of the acoustic discontinuity with time, reduces the source term i.e. flame movement itself has a stabilising effect.

For the limit cycle test case (3), the Rayleigh source term is shown in Figure 5. Again, the changes induced by altering the position of the flame-induced discontinuity are clearly seen, with accounting for flame movement (about the correct spatial-mean position) again showing a stabilising effect.

To demonstrate that accounting for the movement of the flame has an effect more generally, rather than just for the specific test cases chosen, we consider a combustor with the same characteristics as in the limit cycle test case, but with downstream combustor lengths ranging from 0.7 m to 1.15 m. The relative errors between the peak amplitude of the $x_b = \overline{x}_f$ and $x_b\,(t) = x_f\,(t)$ simulations are shown in Figure 6. This confirms that the movement of the discontinuity can induce large changes in limit cycle amplitude across a range of conditions.

Conclusion

Because the flame is compact when compared to the acoustic wavelength scale, changing the position of the flame-induced discontinuity had previously not been attempted in anchored ducted–flame model implementations. However, it has been shown in this paper that applying the discontinuity at the steady spatial-mean

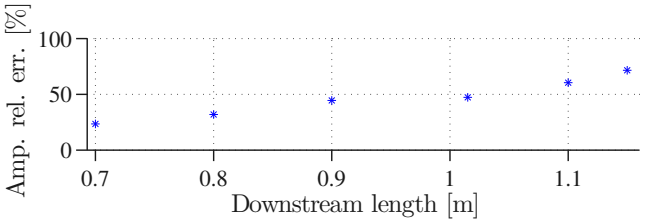

Figure 6: Relative difference between the $x_b = \overline{x}_f$ and $x_b\,(t) = x_f\,(t)$ model peak amplitudes.

position of the flame, or better yet taking into account the time variation of the average flame position, leads to changes in the modes, stability and limit cycle amplitude of the system. This is due to a more accurate modelling of the pressure and heat release phase relationships, which is essential for an adequate modelling of combustion instabilities.

References

[1] Swaminathan, Nedunchezhian & Bray, K.N.C.: Turbulent Premixed Flames, chapter 3. Cambridge University Press (2011)

[2] Fleifil, M. & Annaswamy, A. M. & Ghoneim, Z. A. & al.: Response of a Laminar Premixed Flame to Flow Oscillations: A Kinematic Model and Thermoacoustic Instability Results. Combustion and Flame **106** (1996), 487-510

[3] Dowling, Ann P.: Nonlinear self-excited oscillations of a ducted flame. Journal of Fluid Mechanics **346** (1997), 271-290

[4] Langhorne, P. J.: Reheat buzz: an acoustically coupled combustion instability. Part 1. Experiment. Journal of Fluid Mechanics **193** (1988), 417-443

[5] Langhorne, P. J.: Reheat buzz: an acoustically coupled combustion instability. Part 2. Theory. Journal of Fluid Mechanics **193** (2011), 445-473

[6] Evesque, S. & Dowling, A. P. & Annaswamy, A. M.: Self-tuning regulators for combustion oscillations. Proceedings of the Royal Society's Journal **125** (2003), 186-193

[7] Dowling, Ann P.: A kinematic model of a ducted flame. Journal of Fluid Mechanics **394** (1999), 51-72

[8] Noiray, N. & Durox, D. & Schuller, T. & al: A unified framework for nonlinear combustion instability analysis based on the flame describing function. Journal of Fluid Mechanics **615** (2008)

[9] Rayleigh, John William Strutt: The Theory of Sound London, Macmillan and co. (1877)

[10] Morgans, A. S. & Karabasov, S. A. & Dowling, A. P. & al: Transonic helicopter noise. AIAA Journal **43** (2005), 1512-1524